CORROSION SCIENCE AND TECHNOLOGY, Vol.23, No.5(2024), pp.393~401 pISSN 1598-6462 / eISSN 2288-6524
[Research Paper] DOI: https://doi.org/10.14773/cst.2024.23.5.393

Formation Mechanism of Freckles on Zn-Al-Mg Coatings and their Influence on Processing Properties

Nils Köpper†, Friedrich Luther and Thomas Koll

Metallic Coatings Dept., Salzgitter Mannesmann Forschung GmbH, Salzgitter, 38239, Germany
(Received January 25, 2024; Revised June 03, 2024; Accepted June 03, 2024)

Zn-Al-Mg hot-dip-galvanized steel sheets exhibit some specific surface phenomena that have not been observed on GI coatings and have only been published to a limited extent. One visually very striking optical appearance has been discussed in the literature under the names “freckles” and “dark spots.” However, only a rough formation mechanism has been described to date. Brisberger *et al.* found foreign particles in the center of the defect that could be considered to be a nucleation seed for a freckle. However, the influence of these occurrences on processing properties has not yet been described. For more detailed information on the formation and cause of freckles, metallographic examinations and laboratory trials were carried out in a hot-dip galvanizing simulator to gain a fundamental understanding of the formation mechanism. Topography and processing properties, such as phosphatability, paint appearance, forming properties, and corrosion resistance, were assessed by various methods. Freckles exhibited locally altered crystallization due to a foreign particle, which has an impact on the Zn-Al-Mg coating itself as well as its complex microstructure. New findings on the formation mechanism were obtained from investigations with our hot-dip simulator, which showed possibilities for controlling these surface phenomena in an industrial environment.

Keywords: *Zn-Al-Mg-coating, Coating defects, Freckles, Dark spots, Formation mechanism*

1. Introduction

In the 90s, zinc-aluminium-magnesium coatings (ZM) were developed in Asia due to their improved corrosion properties and were initially mainly used for construction or agricultural applications [1,2]. During the development of the lower alloyed European zinc-aluminium-magnesium coatings and within the scope of the investigations in the VDEh working group, further positive properties of these coatings were determined [3,4]. Especially in the alloying range between 1 % and 3.7 % for Al and Mg respectively, very good properties were found for all important processing steps in the automotive sector. Forming, joining, and painting properties were at least on the level of the established galvanising iron (GI) coatings [5,6]. In particular, the low abrasion during forming and thus less downtime in the press shop was an important argument for establishing the coating in the automotive sector. This made ZM coatings a good alternative, especially in the field of exposed surface applications.

†Corresponding author: n.koepper@sz.szmf.de

However, for exposed applications, a defect-free surface is crucial. A few new surface phenomena have been identified in ZM coatings. These result either from the high oxygen affinity of the alloying elements, or the multiphase solidification of the coating. One of these phenomena is the formation of “freckles” on the strip surface, already observed by Brisberger *et al.* [7]. This is an optical phenomenon on the surface, which is visually perceptible as a round dark spot. According to Brisberger *et al.* the freckles are caused by external germs hitting the still liquid strip surface before solidifying of the coating.

The aim of this study was to evaluate the causes of freckles in more detail and to investigate the processing characteristics of the ZM coating exhibiting freckles.

2. Defect Analysis

Freckles are round appearances on the sheet surface with a diameter of 1-7 mm depending on the solidification conditions. Directly after galvanising, the freckles are shiny and then darken faster than the surrounding surface within a few days and acquire their characteristic brownish

colour. Fig. 1 shows some examples of typical freckles.

The skin passed surface of freckles does not show differences in local roughness to the rest of the material. The shinier structure is explained by a smoother solidification structure of the surface as can be seen in Fig. 2.

Fig. 3 shows a freckle after a FIB section. A foreign particle seems to have adhered to the surface and penetrated the liquid coating to a small extent after the strip leaving the zinc pot. In the cross-section part of the FIB, the primary crystal is surrounded by the eutectic, nucleating from the surface. This agrees with the following theory: First the primary crystals solidify,

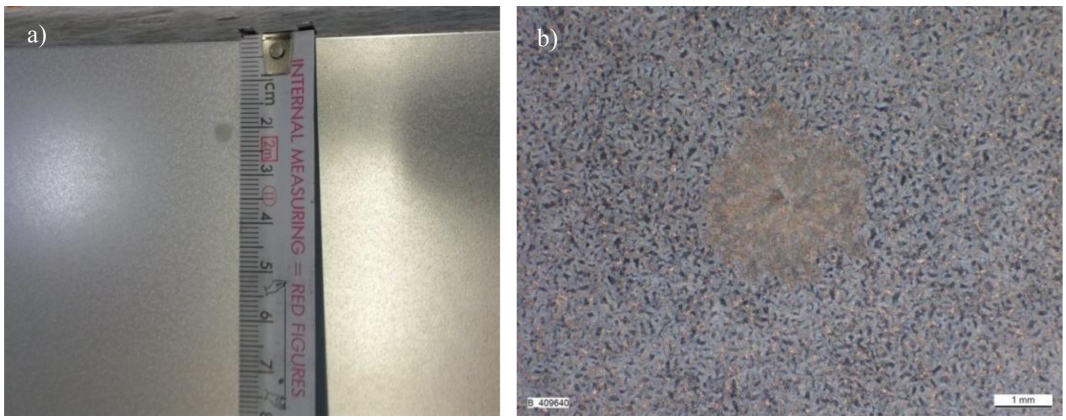

Fig. 1. Image of a typical freckle directly after galvanising (a) and a light microscopic image of a darkened freckle some days after galvanising (b)

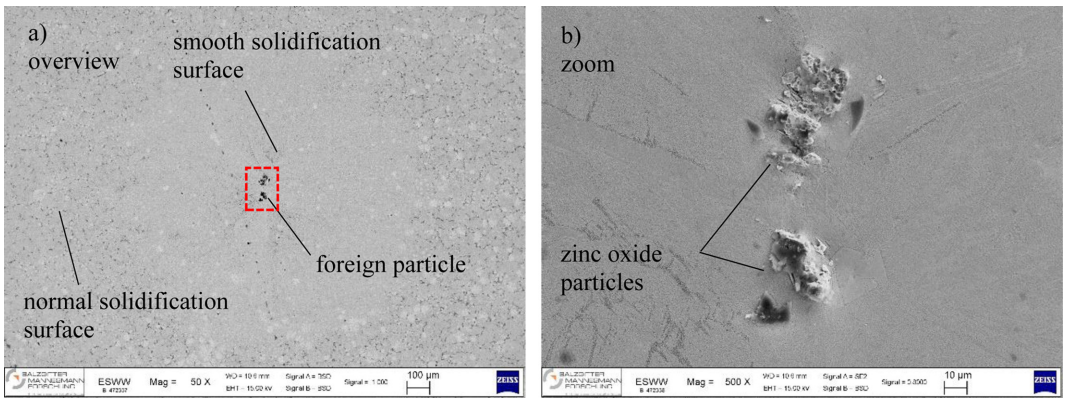

Fig. 2. Overview SEM images of a freckle (a) with a smooth solidification surface and a zinc oxide particle in the centre which is shown in detail (b)

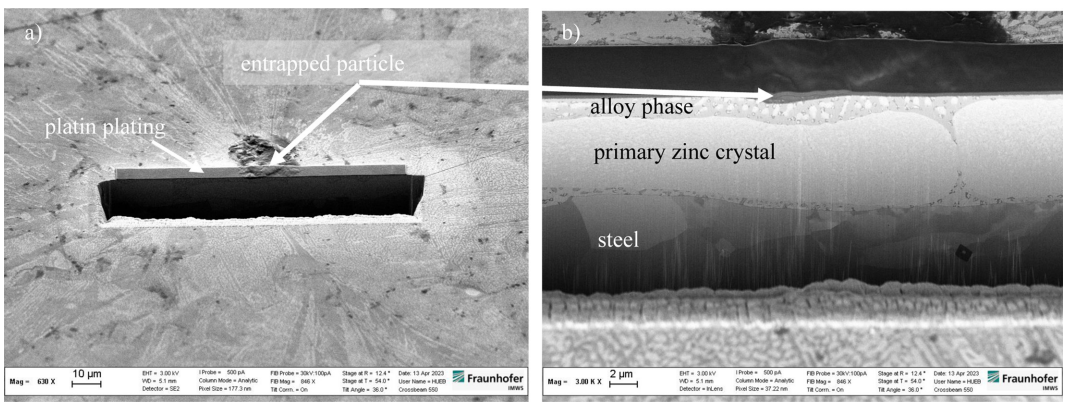

Fig. 3. SEM images of a freckle after a fib cut through the centre particle: a) contrast for top view, b) contrast for cross section view

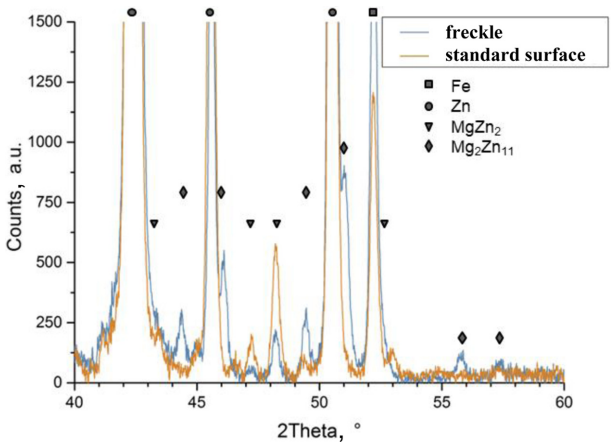

Fig. 4. Comparison of the lattice structures of a freckle and the surface surrounding it in XRD-diffractometry

starting their nucleation from the interface and then growing laterally to an extent several orders of magnitude bigger than the coating thickness. During or after this process the eutectic solidifies, starting from the seed at the surface in its altered crystal structure. This could be identified as Mg_2Zn_{11} by X-ray diffraction, see Fig. 4. In the top view, clear solidification patterns of the eutectic can be seen, originating from the particle situated in the centre of the freckle. At the corner between cross section and surface one can see the correlation between both views of the eutectic. Again, this pattern extends to several orders of magnitude larger than the coating thickness and gives a hint of the size of the different crystal structure, generating the so-called freckle. Such large crystal sizes are made possible by local premature solidification caused by a nucleation seed.

The Mg_2Zn_{11} phase is the thermodynamically stable phase that would be expected in ZM coatings according to the phase diagram but is usually not been observed in the standard coatings [8,9].

3. Experimental Method

To gain a better understanding of the formation of freckles, an attempt was made to produce freckles in a hot-dip galvanising simulator. Previous publications indicate that freckles are induced by external nuclei [7]. For this purpose, a cold-rolled interstitial free (IF) steel with a thickness of 0.8 mm was galvanised in the hot-dip simulator. A typical hot-dip galvanising cycle was used, as the annealing process plays no important role in the formation of freckles. The samples were annealed in 4 % HNx atmosphere and heated at 10 K/s to 830 °C. Subsequently, the samples were maintained at this temperature for 115 s and then cooled to 450 °C at 30 K/s. The overaging time was 80 s. The samples were then immersed in the ZM bath for 5 s with a composition of 1.7 % Al and 1.1 % Mg. The coating gauge was adjusted to 20 µm with a wiping nozzle and the sample was moved to the cooling zone. There it was cooled down to 300 °C without active cooling. In order to bring external seeds

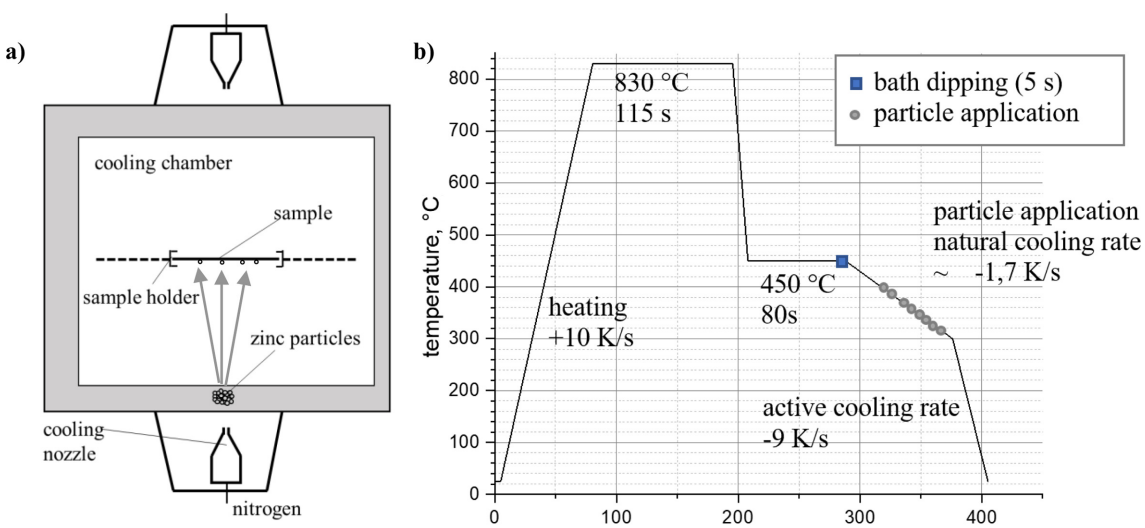

Fig. 5. Experimental set-up in the cooling zone of the hot dip simulator (a). Annealing cycle used in the hot dip galvanising simulator with the times of seed application in the cooling zone (b)

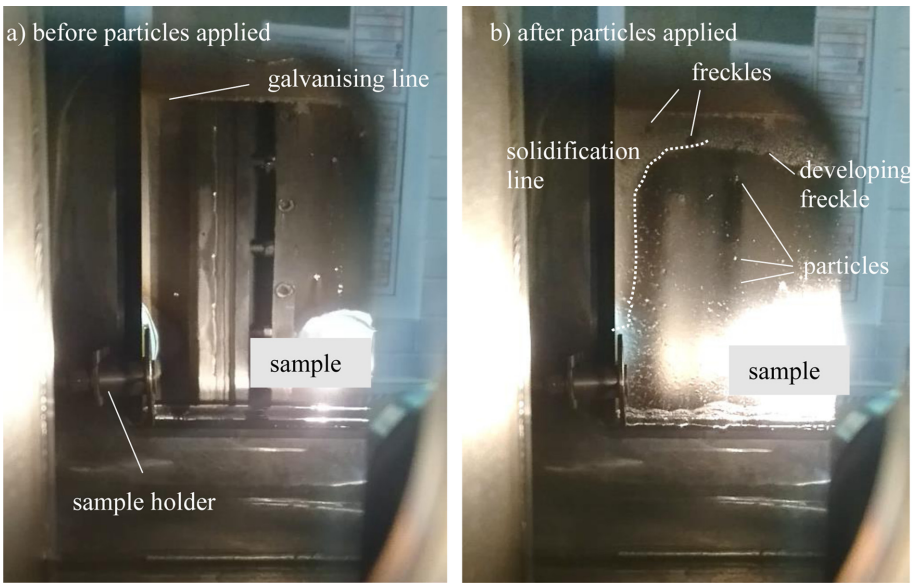

Fig. 6. Photos of a sample in the cooling zone of the hot dip simulator a) before and b) after application of foreign particles with incipient solidification

Table 1. Composition of the zinc sublimate determined by XRD

Compound		ZnO	Zn
Zinc sublimate	wt%	98,4	1,6

onto the liquid surface, some particles were placed in front of the cooling nozzle of the hot dip simulator as shown in Fig. 5. With a short cooling blast at different sample temperatures in the range between 400 °C and 320 ºC, these particles were blown onto the liquid sample surface. This process does not significantly affect the temperature of the samples. From 300 °C the solidified sample was cooled to room temperature at 9 K/s.

Zinc sublimate was used as foreign particles for the experiments. The powder was sieved to < 63 µm and the composition is shown in Table 1.

Fig. 6 shows the view into the hot-dip simulator through windows in the cooling zone, before and after the particles were blown onto the sample.

4. Results and Discussion

The emergence of freckles could be reproduced in our hot-dip galvanising simulator by applying powder onto the liquid coating. The formation of the resulting freckles could be recorded, as can be seen in Fig. 7.

The growth of the freckle in the sample centre (see arrow) begins before the coating solidifies completely and takes about 3 s to grow to a size of 7 mm with a natural cooling rate of approx. 1.7 K/s. Fig. 7 shows the movement of the solidification line moving across the sample in the direction of the freckle. The premature crystallisation of the freckle already expected from the analysis could thus be shown.

The temperature at which those particles are applied to the sample has a significant influence on the formation of freckles. Very few freckles could be detected already on samples without applying matter before solidification. This is probably due to a small amount of particles that is unavoidably present in the simulator. Applying particles at temperatures up to 380 °C induced significantly more freckles. Interestingly, applying particles at temperatures equal or higher than 390 °C generates much less freckles.

Consequently, the impact of a foreign particle onto the surface on its own is not sufficient for the formation of a freckle. This particle must hit the surface in a certain phase of solidification to trigger a premature nucleation. ZM coatings do not exhibit a solidification point, but rather a solidification interval, caused by a complex multi-phase solidification that depends on the composition of the bath. The solidification path of the considered ZM coatings may yield during serial production – depending on bath composition – some of the following phases – a primary zinc phase, a binary $MgZn_2$/Zn- phase and a ternary Zn/Al/$MgZn_2$-phase.

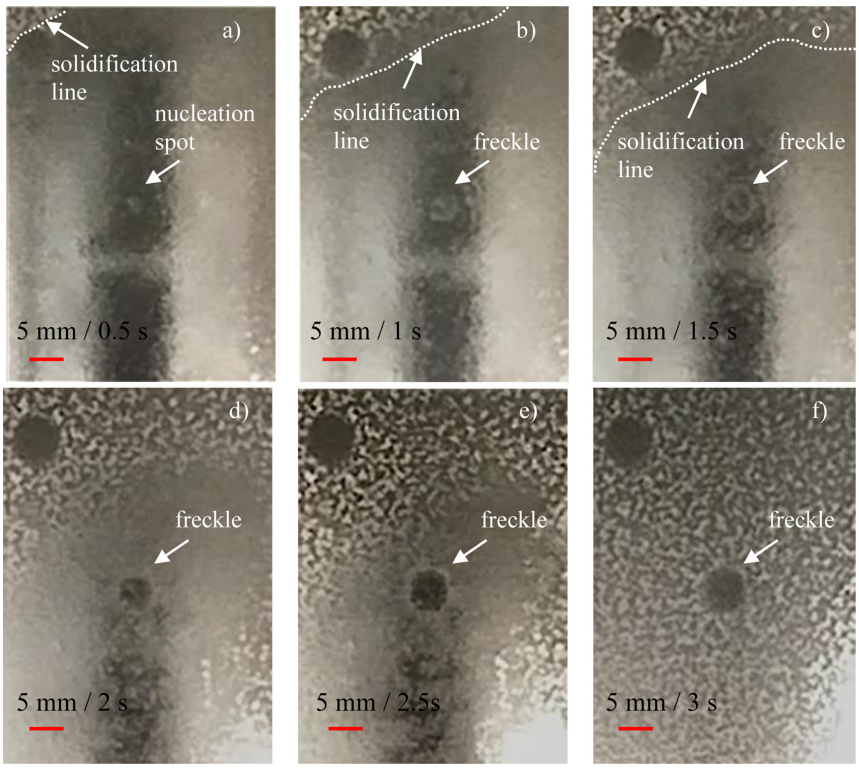

Fig. 7. Photographs of the growth of a freckle from a foreign nucleus on the liquid surface to a size of 7 mm within 3 s (a-f) during solidification of the Zn-Al-Mg-coating

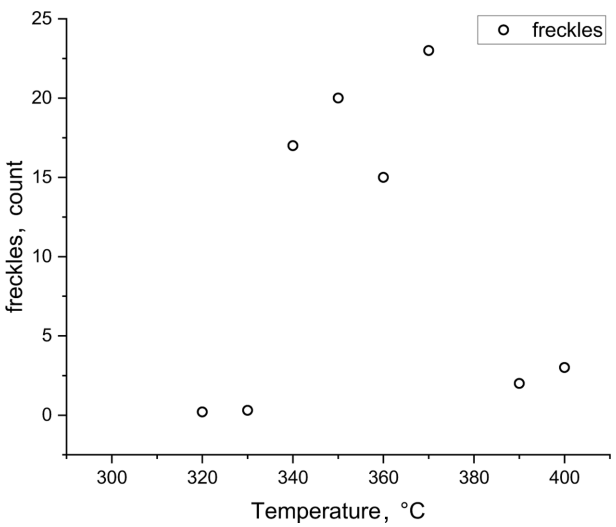

Fig. 8. Number of freckles on the sample as a function of the temperature at which powder is applied to the sample surface

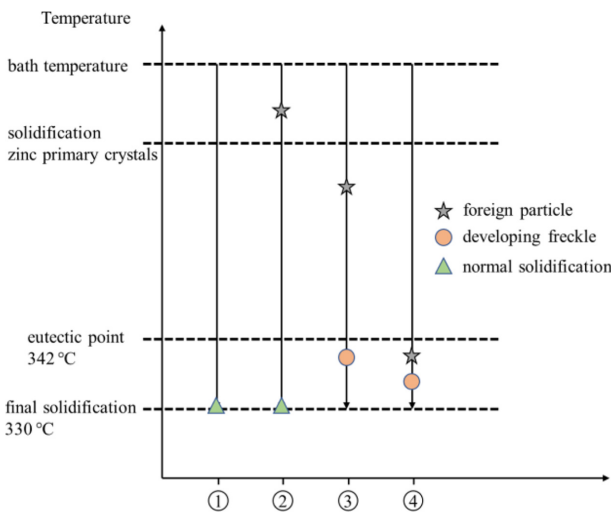

Fig. 9. Four schematic sequences of different solidification paths with and without freckle formation depending on the temperature at which a foreign particle hits the liquid surface

At 342 °C the eutectic point is reached and the remaining coating solidifies in the form of a ternary eutectic. The temperature range in which a freckle is triggered by external particles indicates that this is only the case when zinc primary crystals have started to form. A possible schematic sequence of freckle formation is shown in Fig. 9.

5. Processing Properties

The extent of a freckle of several millimetres enables to examine locally differing processing properties on one sample, whether produced in a production line or in the lab. Feature and reference state have experienced identical process parameters throughout all production steps. This is especially relevant for processing properties, where both substrate and surface play a role, e.g. in forming. The downside of the small extent of the individual freckles is the fact that investigations in need of larger feature areas may not be possible, like a local friction coefficient or local abrasion.

In the following processing properties like forming and painting as well as corrosion protection are investigated.

5.1 Forming

The forming properties of the freckles were tested in different loading scenarios. For analysis, a drawing test with a hemispherical punch, strip drawing tests (flat and round die) and 3-point bending tests were conducted. In all tests, the freckle was positioned in such a way that it was exposed to a high load and could be compared with the surrounding areas. In all cases, no differences were observed between the areas with and without freckles, neither in friction tests nor in tests with induced elongation. In the following, the elongation was tracked using the ARAMIS system and the area with a freckle was marked in grey. There were no differences in elongation to the surrounding material. Fig. 10 shows the elongation after the deep drawing process with a depth of 70 mm and a speed of 1.2 mm/s. No significant difference was found between the freckle and the surrounding surface.

In addition to the deep-drawing tests, the influence of friction on the freckle was investigated. Therefore, a strip drawing test with a flat and round die was used. The sample coupons were drawn 5 times with velocity of 15 mm/s and a normal force of 5 kN. The draw length was 85 mm for the first stroke and 80 mm for the following strokes without re-oiling. Fig. 11 shows a sample after the strip drawing test. The previously clearly visible freckle is barely visible after the examination. In the SEM image, no difference in the areas with and without freckles could be observed. The pretex structure from the skin-passing process is slightly levelled, but still visible in both cases.

Fig. 12 shows SEM images of a 90° bending angle after a 3-point bending test based on VDA238-100: 2020-07 with a bending radius of 0.4 mm, looking at areas without (a) and with (b) freckles.

In both areas, fine cracks can be seen in the coating along the bending edge. Significant differences between the two areas are not visible. No differences can be seen in the other mentioned deformations either. Concerning forming applications, no significant differences could be found between the areas with and without freckle in any of the mentioned test geometries.

5.2 Painting and Corrosion

Painting properties of the surfaces were also checked

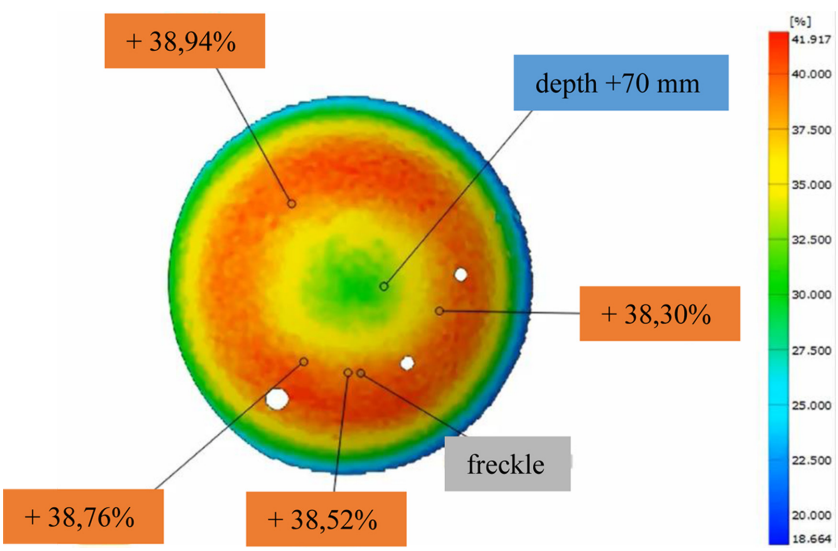

Fig. 10. On the hemispherical sample, the elongation was observed using the Aramis system

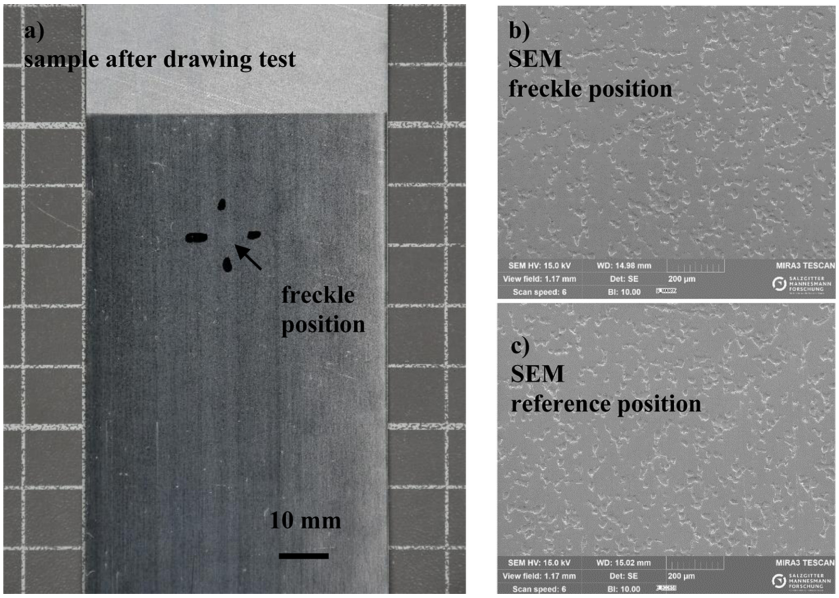

Fig. 11. Images of a sample after the strip drawing test. The freckle is barely visible. In the light microscope images, the areas with (b) and without (c) freckles show comparable surfaces

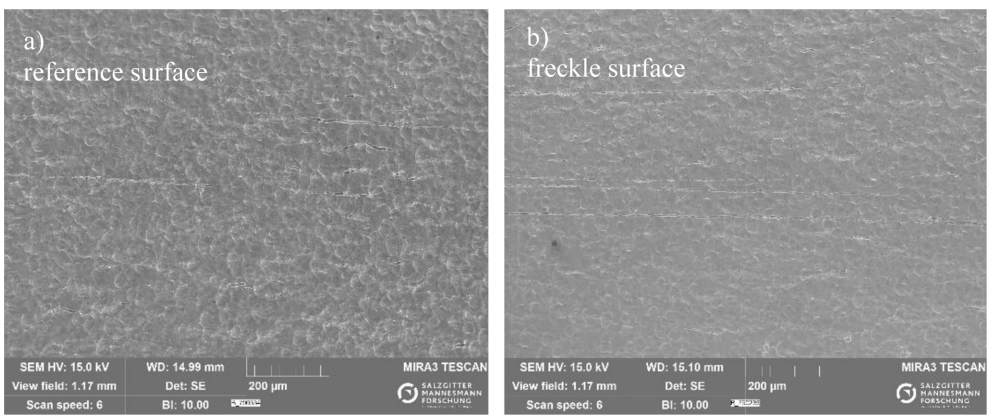

Fig. 12. SEM image of the outer bending radius of the reference (a) and freckle (b) position with 90° bending angle

in comparison with the reference state. The idea for the paint and corrosion tests was to use samples exhibiting freckles and compare the behaviour of areas with and without freckles directly. In addition, after cathodic dip coating, it was visually checked whether the freckles were still visible after painting. For this purpose, defect foils were created in order to track the exact positions of the freckles after painting. First the surface was phosphated (Gardobond 26 TA) under typical automotive conditions and then painted with a cathodic dip coating (CarthoGuard® 800).

Fig. 13 shows the freckle before and after phosphating. After phosphating, it remains visible in the microscope, although its brownish contrast has decreased significantly.

While the freckle to the right of the scratch is still visible as a dark area in the light microscopic image, there is no difference between the area with and without freckles in the SEM image. The phosphate crystals also do not show any differences, neither in composition nor in crystal form.

After phosphating (Fig 14), the samples were painted with a typical automotive cathodic dip coating with a layer thickness of approx. 20 µm. The freckles were no longer detectable visually after coating. Consequently, no differences were found in the paintability of the freckles.

The e-coated samples were subsequently tested in a cyclic corrosion test according to VDA233-102 for 6 weeks. Prior to the corrosion test, one Clemen scribe (down to zinc), and one Sikkens scribe (down to steel)

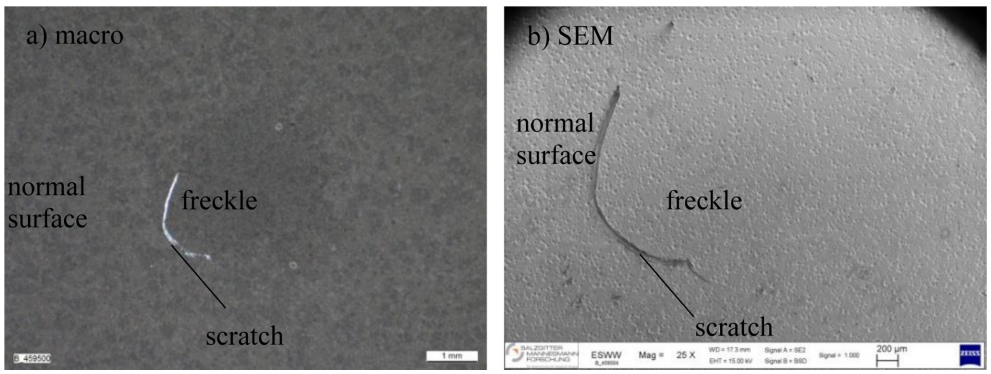

Fig. 13. Light microscopic image of a phosphated freckle (a) with the corresponding SEM image (b)

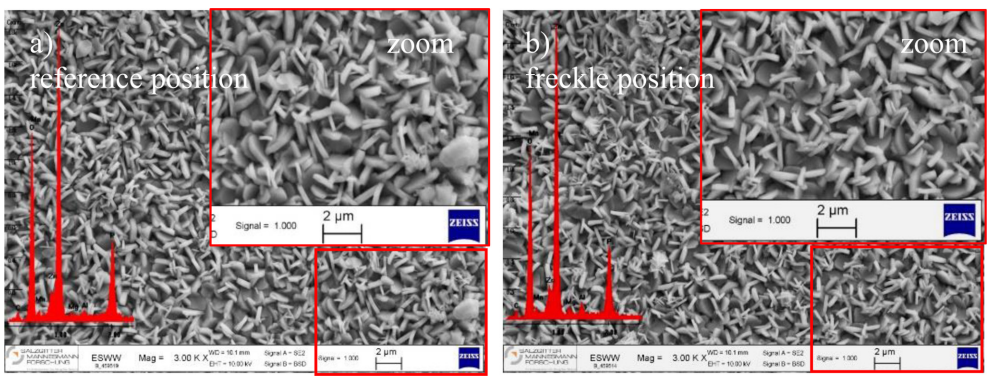

Fig. 14. Phosphate crystal morphology and EDX spectra exhibit no differences between the reference (a) and the freckle (b) position

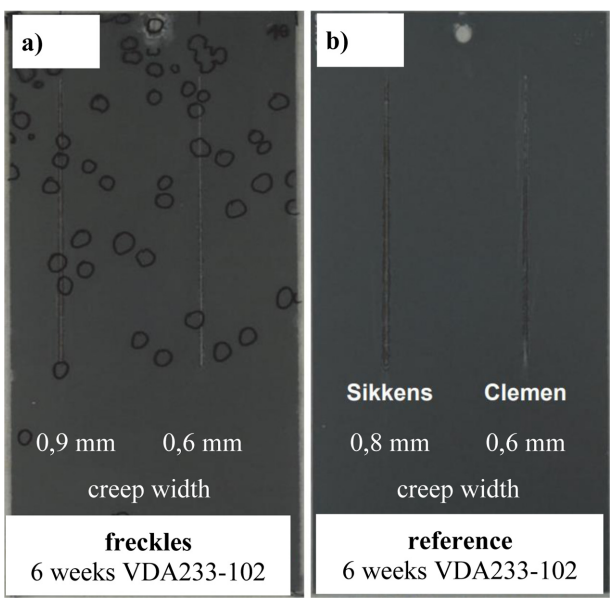

Fig. 15. Comparison of scribe corrosion creep (a) Sikkens (to steel) and b) Clemen (to zinc) after 6 weeks cyclic corrosion test according to VDA 233-102:2013

with a width of 0.5 mm were applied to each of the sample surfaces. The scribes were placed so that they ran through several freckles. Subsequently, the corrosion creep width was evaluated in comparison with and without freckles. To find the original position of the freckles again after the corrosion test, a defect foil was created before e-coating. After the corrosion test the creep width of the e-coated samples in the areas with and without freckle is comparable (Fig. 15).

6. Conclusion

The surface phenomenon freckles could be successfully reproduced in our hot-dip galvanising simulator. It was demonstrated that the formation of freckles is initiated by an external nucleus. However, it could be shown that the altered nucleation only takes place in a narrow temperature range. In addition, the formation of freckles could be observed directly by camera. The freckles crystallise before complete solidification of the coating. Less undercooling of the melt is observed in this area.

The metallographic analysis showed a very smooth solidification structure in the area of the freckle. However,

roughness is not affected, as the skin pass structure penetrates much deeper into the material.

The investigated processing properties do not show any differences compared to the surrounding surface. The freckles can be formed, phosphated and painted without restriction. No differences were found in the corrosion tests carried out either.

References

1. K. Atsushi T. Takao, *Hot-Dip Zn-Al-Mg Coated Steel Sheet excellent in Corrosion Resistance and Surface Appearance and Process for the Production Thereof*, Nisshin Steel Co. ltd., EP0905270 (1997.12.12).
2. H. Shindo *et al.*, *Proc. 4th International Conference on Zinc and Zinc Alloy Coated Steel Sheet (Galvatech 1998)*, p. 437, Iron and steel institute of Japan, Makuhari, Chiba, Japan (1998).
3. W. Fischer *et al.*, *Proc. 9th International Conference on Zinc and Zinc Alloy Coated Steel Sheet (Galvatech 2013)*, p. 632, The Chinese Society for Metals, China (2013).
4. W. Fischer *et al.*, *4th International Conference on Steels in Cars and Trucks*, p. 516, Steel Institute VDEh, Germany (2014).
5. T. Koll *et al.*, *Proc. 9th International Conference on Zinc and Zinc Alloy Coated Steel Sheet (Galvatech 2013)*, p. 625, The Chinese Society for Metals, China (2013).
6. J. Schulz, F. Vennemann, G. Nothacker, *Proc. 10th International Conference on Zinc and Zinc Alloy Coated Steel Sheet (Galvatech 2015)*, p. 153, Association for Iron & Steel, Canada (2015).
7. R. Brisberger, H. Vasold, H. Antrekowitsch, *Proceedings of European Metallurgical Conference MC*, p. 775, GDMB Society for Mining, Germany (2011).
8. J. P. Mogeritsch, A. Ludwig, B. Böttger, G. Angeli, C. K. Riener, R. Ebner, *Proc. VII International Conference on Computational Methods for Coupled Problems in Science and Engineering Coupled Problems*, p. 1171, International Centre for Numerical Methods in Engineering, Greece (2017). https://smmp.unileoben.ac.at/fileadmin/shares/unileoben/smmp/docs/C161_Coupled_Problems_in_Science_and_Engineering_VII.pdf
9. Z. Zhang, J. Zhang, X. Zhao, X. Liu, X. Cheng, S. Jiang, and Q. Zhang, Effect of Al/Mg Ratio on the Microstructure and Phase Distribution of Zn-Al-Mg Coatings, *Metals*, **13**, 46 (2023). Doi: https://doi.org/10.3390/met13121963